Entanglement Transitions in One Dimensional Confined Fluid Flows

Kenneth Millett *
Eleni Panagiotou †

September 12, 2016

Abstract

The strength of entanglement present in a tubular structure consisting of short vortex flow filaments is assessed using a periodic boundary condition (PBC) model by employing the magnitude of the eigenvalues of the periodic linking matrix associated to the filamental structure. The effects of tube radius and of the alignment of the filaments on the strength of entanglement are shown to suggest that strongly aligned flow systems exhibit a stronger entanglement than those consisting of randomly aligned filaments of the same density.

1 Introduction

The objective of this study is to illuminate the consequences of spatial constraints on a filamental vortex flow structure contained in a long tube, see Figure 1. arising from the cross sectional geometry of a tube and from the spatial alignment constraints acting on filamental structures of a fluid flow or aligning constraint of varying strength. While this study focuses on linear tubes, these methods apply to more complex circumstances such as knotted vortex tubes [3]. We employ a course grained periodic boundary condition (PBC) polygonal simulation model to quantify or characterize the resulting entanglement of the flow filaments. The one dimensional periodic boundary constraint tube model employs a circular cross-sectional geometry. The radius of the cross-sectional disc varies from $\frac{1}{5}$ the edge length of the chain to 5 times the persistence length of the vortex flow trajectories. In addition to the scale of the tube constraint, we apply a varying constraint that causes the spatial alignment of the polygonal edges of the modeled conformation to vary from those of a random, disordered, filament to those of a chain that is increasingly monotonically aligned to become almost parallel to the tube axis.

*Department of Mathematics,University of California, Santa Barbara, CA 93106, USA
†Department of Mathematics,University of California, Santa Barbara, CA 93106, USA

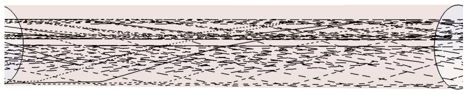

Figure 1: A simulated filamental structure in a tube.

To quantify the spatial extent of the filamental structures, we estimate the mean radius of gyration and the mean end-to-end length. The degree of entanglement of the filaments is measured using Panagiotou's periodic linking number and self-linking number [5, 7, 4]. The complexity of the system is quantified by using one, two, and finally, three independent filaments to generate the PBC system, determine associated periodic linking matrices and the resulting periodic linking eigenvalues [6]. These define new measures of the entanglement that arise as a function of confinement and alignment constraint and illuminate the structural transitions.

2 Confined Fluid Flows via Periodic Boundary Condition (PBC) Models

The underlying structure of the *Periodic Boundary Condition*, PBC, model employed in this study consists of solid right cylinder whose x length is one and whose y and z coordinates lie within a disc of radius $a > 0$ and containing a collection of arcs whose endpoints either lie in the interior or intersect the $x = 0$ or $x = 1$ faces under the constraint that the pattern on both faces is identical. The later condition allows one to create and infinite structure by taking the union of integer translates of the cells and taking the unions of the resulting chains to define a collection of one dimensional chains. As, in general, these chains may be non-compact, we will require that each chain has precisely the same number of edges, N, thereby imposing an aspect of homogeneity. Due to the PBC structure, there is also a large scale homogeneity in the collection of chains that we interpret as encoding flow lines in a fluid flow or, if one wishes, a collection of macromolecules. One can understand, in the later case, the edge length as representing a Kuhn length, [2], of the macromolecule. The radius of the cross-sectional disc should be understood in terms of this Kuhn length, or persistence length, and influencing the character of the flow or the gel being modeled. We are also interested in the consequences of increased alignment of the incremental structural segments and, therefore, will study these structures as they are subjected to a wide range of alignment constraints ranging from none, random alignment, to very strong influences resulting in a monotone, but not constant, directional orientation of the filaments. In one case, the structure is quite chaotic while, in other cases, the structure is elongated. In all cases, however, one observes a quantifiable degree of entanglement between the substructures. In the next section, we will describe how we propose to quantify the degree of entanglement.

3 Periodic Linking Entanglement in Confined Structures Modeled using Periodic Boundary Conditions

The linking number between two oriented chains, l_1 and l_2, is defined using parameterizations of the chains, $\gamma_1(t)$ *and* $\gamma_2(s)$, via the Gauss linking integral:

Definition 3.1. The Gauss *linking number* of two disjoint (closed or open) oriented curves l_1 and l_2, whose arc-length parameterizations are $\gamma_1(t), \gamma_2(s)$ respectively, is defined as a double integral over l_1 and l_2 [1]:

$$L(l_1, l_2) = \frac{1}{4\pi} \int_{[0,1]} \int_{[0,1]} \frac{(\dot{\gamma}_1(t), \dot{\gamma}_2(s), \gamma_1(t) - \gamma_2(s))}{||\gamma_1(t) - \gamma_2(s)||^3} dtds, \tag{1}$$

where $(\dot{\gamma}_1(t), \dot{\gamma}_2(s), \gamma_1(t) - \gamma_2(s))$ is the triple product of $\dot{\gamma}_1(t), \dot{\gamma}_2(s)$ and $\gamma_1(t) - \gamma_2(s)$.

In a PBC model, each chain is translated to give an infinite collection copies of itself, see Equation 2. As a consequence, one is faced with quantifying the linking of one chain, l_0, with infinitely many translation copies of itself, l_v, or with infinitely many copies of another chain. This is achieved by employing Panagioutou's [4] periodic linking and self-linking numbers described next.

$$l_v = l_0 + \vec{v}. \tag{2}$$

3.1 The periodic linking number

In a periodic system we define linking at the level of free chains, i.e. the collections of translation copies of chains, l_0 or J_0. See [4] for a discussion of the motivation for the following definition. The underlying idea is to calculate the linking between the generating chain in one with all the chains in the other free chain.

Definition 3.2 (Periodic linking number)**.** Let I and J denote two (closed, open or infinite) free chains in a periodic system. Suppose that I_0 is an image of the free chain I in the periodic system. The *periodic linking number*, LK_P, between two free chains I and J is defined as:

$$LK_P(I, J) = \sum_{\vec{v} \neq \vec{0}} L(I_0, J_0 + \vec{v}), \tag{3}$$

where the sum is taken over all the images of the free chain J in the periodic system.

The periodic linking number has the following properties with respect to the structure of the cell, see [4], which follow directly by its definition:
(i) The infinite sum defining LK_P converges, i.e. LK_P makes sense mathematically.
(i) LK_P captures all the linking that all the images of a free chain impose to an image of the other.
(ii) LK_P is independent of the choice of the image I_0 of the free chain l in the periodic system.
(iii) LK_P is independent of the choice, the size and the shape of the generating cell.
(iv) LK_P is symmetric.

3.2 The periodic self-linking number

The quantification of the linking of a free chain with itself is a bit special and requires a bit more care as there are two contributing cases, the linking of a chain with itself and the linking of a chain with translations of itself. As a consequence, one is lead to the following definitions [4]:

Definition 3.3 (Self-linking number)**.** Let l denote a chain, parameterized by $\gamma(t)$, then the *self-linking number* of l is defined as:

$$\begin{aligned} Sl\,(l) \quad &= \tfrac{1}{4\pi}\int_{[0,1]^*}\int_{[0,1]^*}\tfrac{(\dot\gamma(t),\dot\gamma(s),\gamma(t)-\gamma(s))}{||\gamma(t)-\gamma(s)||^3}dtds \\ &\quad +\tfrac{1}{2\pi}\int_{[0,1]}\tfrac{(\gamma'(t)\times\gamma''(t))\cdot\gamma'''(t)}{||\gamma'(t)\times\gamma''(t)||^2}dt. \end{aligned} \tag{4}$$

The self-linking number consists of two terms, the first being the Gauss integral and the second being the total torsion of the curve.

Definition 3.4 (Periodic self-linking number)**.** Let l denote a free chain in a periodic system and let l_u be an image of l, then the *periodic self-linking number* of l is defined as:

$$SL_P(l) = Sl(l_u) + \sum_{v\neq u} L(l_u, l_v), \tag{5}$$

where the index v runs over all the images of l, except l_u, in the periodic system.

As with the periodic linking number, the mathematical proof of its existence of this quantity and its properties are proved in [4].

3.3 The periodic linking matrix

In order to analyze the linking entanglement present in our PBC system, L, consisting of a finite number of free chains, $l_1, l_2, ..., l_n$, we employ an $n\ x\ n$ real symmetric matrix, LM, the *periodic linking matrix* [6] whose i,jth entry is defined by equation

$$
\begin{aligned}
LM_{i,i} &= SL_P(l_i) \\
LM_{i,j} &= LK_P(l_i, l_j)
\end{aligned}
\tag{6}
$$

In the case of a single generating chain, I, the periodic linking matrix consists of a single entry, the periodic self-linking number, $SL_P(I)$. From the definition, there are two contributing factors, the self-linking given by the equation 5 and the linking between distinct copies, reflecting distinct features of periodic self-linking.

For systems with two independent chain types, the periodic linking matrix adds entanglement information due to the linking between the two distinct chains. Associated to the periodic linking matrix are two real eigenvalues, $e_1(L)$ and $e_2(L)$, given in decreasing order. The larger of these, $e_1(L)$ is proposed as the dominant characterization of the linking entanglement of the PBC system. The set of eigenvalues is the *periodic linking spectrum* of the system.

Similarly, for systems with n independent chain types, one defines the periodic linking matrix, LM. The associated ordered collection of eigenvalues, $e_1(L), ..., e_n(L)$ define the spectrum of the PBC system.

4 Simulation of One Dimensional PBC Systems

In this study we generate polygonal chains having a variety of spatial characteristics. These chains have unit length edges and are required to lie within tubes with disc cross-sections of radius varying from 0.1 to 5. The initial end of the segment is chosen, randomly, to lie in the generating cell and edges are sequentially selected to construct a chain of length 25 to lie within the tube according to physical characteristics of the model. These generating chains, in collections of an individual chain, two independent chains, or three independent chains are then extended by integral translations to determine the one dimensional PBC conformation.

The physical models considered here are
(1) In the *random model*, edges are randomly selected subject to the constraint of lying within the tube. (2) In the *parameterized alignment model*, edges are selected to lie within a parameterized cone of alignment directions subject to the constraint of lying within the tube and with increasing probability of lying in the positive direction cone.
In both cases, the intersections of the chain with the positive and negative faces of the cell are identical, the being the PBC requirement that allows the continuation of the chain to adjacent cells.

4.1 Polygonal Chains

The desired filamental structure is modeled using polygonal chains of unit edge length in a PBC system. The *diameter* of a chain is the maximum distance between vertices of a connected component of the system. The *squared radius*

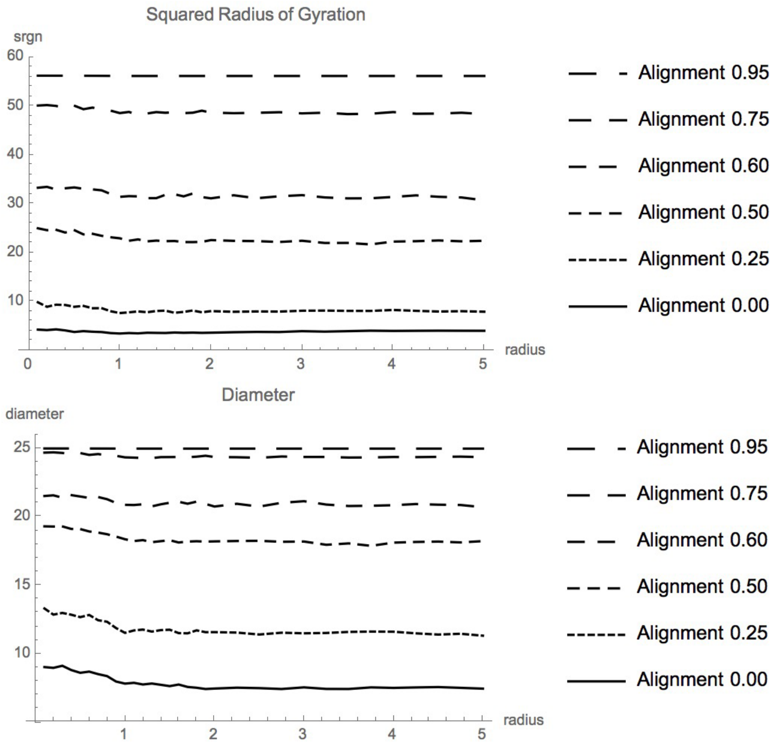

Figure 2: The mean squared radius of gyration and diameter of 25 step chains as a function of the tube radius and alignment constraint

of gyration, $srgn(C)$, of a chain, C with $n+1$ vertices $\{v_1, \ldots, v_{n+1}\}$ of a connected component of the system is defied as follows:

$$cm(C) = \frac{\sum_{i=1}^{n+1} v_i}{n+1} \tag{7}$$

$$srgn(C) = \frac{\sum_{i=1}^{n+1} (v_i - cm(C))^2}{n+1} \tag{8}$$

4.2 An Example

In Figure 4 we show a simple example of a single length 25 chain contained in a PBC tube whose cross-sectional disc of radius 1 under an alignment constraint scaled to 0.00 and to 0.50. For this filamental structure, we systematically study a range of lengths, tube cross-sections, and scaled alignment constraints

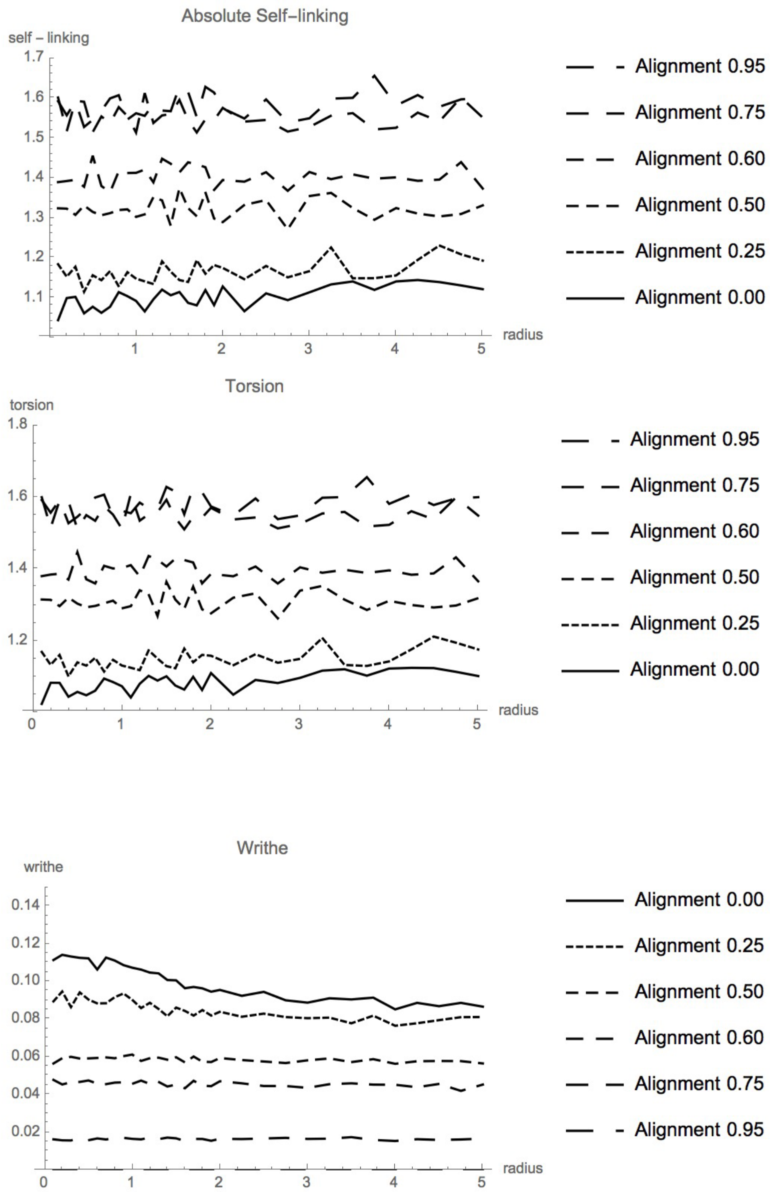

Figure 3: Absolute self-linking, torsion and Gaussian writhe components of single 25 step chains as a function of alignment and constraint

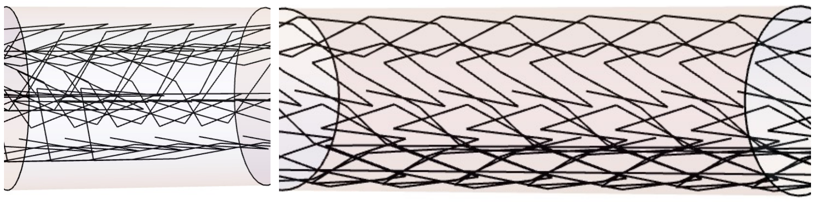

Figure 4: PBC Examples: unit radius disc cross-section, single chain of length 25. Left, 0.00 alignment constraint (random) and, second, 0.50 alignment constraint.

to estimate how the fundamental parameters of shape and entanglement depend upon them.

4.2.1 Effect of Tube Cross-Section Variation

To visually illustrate the effect of the radius of the disc cross-section, we consider a family of length 25 chains subjected to an alignment bias of 0.25 having radii of 0.25, 0.5, 0.75, 1.0, 5.0, and 10.0, see Figure 5. In these, one can observe the increasing freedom of spatial exploration that is provided by increasing the radius of the tube.

4.2.2 Effect of Scaled Alignment Constraint

The scaled alignment constraint varies from 0.00, corresponding to a uniform random distribution, to 1.00 corresponding constant direction aligned to the tube axis giving a straight 'rod like' result. The consequence of the variation is illustrated, Figure 6, for a tube of radius 0.25 with alignment constraint 0.00, 0.25, 0.50, 0.75 and, 0.95. In these, one can see the strong consequence of an alignment preference as the chain evolves from a random one to one that is visually approaching that of a straight rod.

4.2.3 Shape and Entanglement Effects

For example, for a sample size of 500 of such random, i.e. 0.0 alignment, chains, we find a mean diameter of 7.86 units with a mean radius of gyration of 3.57. The mean absolute self-linking is 1.09. As a measure of entanglement, we find the mean maximal, medial, minimal absolute eigenvalues of the linking matrix to be 1.18, 1.01 and, 0.46 respectively. In contrast, for a sample with an alignment bias of 0.50, one has a mean diameter of 18.35 with a radius of gyration of 22.77 and a mean absolute self-linking of 1.34. The absolute eigenvalues have means of 2.20, 1.27, and 0.57 respectively. The increased level of entanglement found in aligned systems compared to a fully random system will be one of the foci of our analysis the filamental structure's dependence upon cross-sectional constraints and alignment.

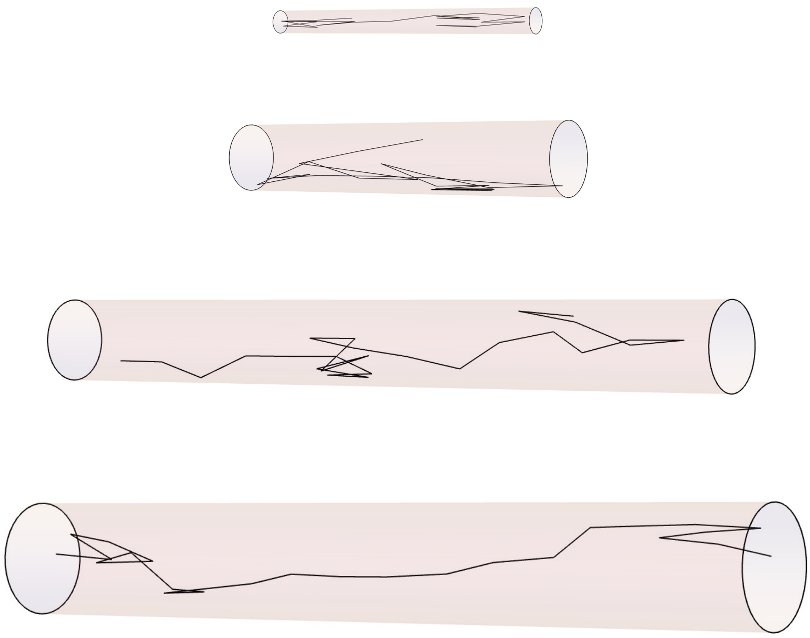

Figure 5: Effect of tubular constraint on length 25 chains (alignment constraint 0.25; tube radius: 0.25, 0.50, 0.75, and 1.00.

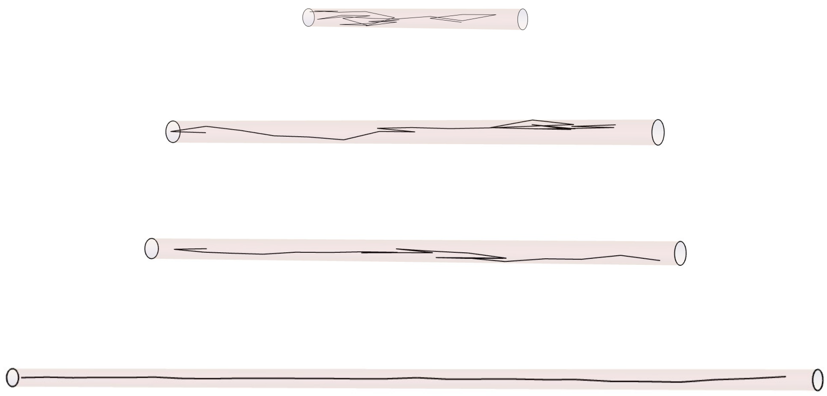

Figure 6: Effect of alignment on length 25 chains in a tube of radius 0.25; alignment scale 0.00, 0.25, 0.50 and, 0.75.

5 Entanglement Effects due to Alignment Constraints and Tube Confinements

The mean individual chain characteristics considered are the radius of gyration, the chain diameter, the self-linking number, and the chain torsion that have been discussed in the previous section. For systems of two or more independent chains, a more complex form of entanglement can occur measured by the mean absolute value of the eigenvalues of the periodic linking matrix ordered by decreasing magnitude.

5.1 Diameter and Mean Squared Radius of Gyration

In Figure 2 we show the effect of the tube radius and alignment constraint on the size of the filament as measured by its mean squared radius of gyration and diameter. Here, one observes that increasing the alignment constraint causes a resulting increase in length of the filament by both measures. Interestingly, the increased tube radius initially causes the scale of the filament to decrease slightly until radius about 1.5 at which point the scale appears to stabilize despite the increase in radius of the tube.

5.2 Linking and Self-linking Numbers

As the chains are piecewise linear, the Gauss integral and the total torsion are determined using extensions of the smooth chain definitions to these chains. With respect to the self-linking of a single chain segment with itself, the mean absolute value of the self-linking number appears to be, up to statistical variation, relatively constant for each alignment value as a function of the radius of the enclosing tube with, perhaps, a slight increase with increasing radius, see Figure 4. The value is smallest for random chains and somewhat larger as the alignment increases. To understand why this is the case, we first consider the total torsion. In our data one observes that this is roughly independent of the radius of the cross-sectional disc with, perhaps, a slight increase with increasing tube radius. The value of the torsion increases with increasing alignment. This is due to the fact that, in the polygonal context, the total torsion is the sum of the angles between two adjacent planes defined by a sequence of three edges in the chain, the first two determine the first plane, the last two determine the second plane. The variation of these angles should be about the same for random chains as it is for strongly aligned chains, but there is an increase with increasing torsion with increasing alignment. Can one explain this? When the alignment constraint is 1.00, the structure is a straight rod and, therefore, with zero torsion. One expects that for any value very close to 1.00, the total torsion will be roughly that shown for 0.75 and 0.95. Why then, is the total torsion value smaller for 0.00 and why is there little variation of total torsion over the changes in cross sectional radius? For cross sectional radius greater than 1.5, we may not expect to see any effects, as it is the case with the diameter and mean squared radius of gyration.

The Gaussian writhe term of the self-linking number shows a decrease with increasing tube radius for random polygons as one would expect due to the decreasing confinement of the chain approaching the asymptotic writhe of an unconstrained chain. As the alignment increases, one expect and, indeed, observes in our data that the Gaussian writhe contribution to the self-linking decreases with increasing alignment and approaches 0 at 0.95. Of the random chain, we observe that this Gaussian contribution decreases with increasing tube radius appearing to approach, asymptotically, the unconstrained chain value.

These contributing factors determine the evolution of the mean absolute self-linking of a single chain. The periodic self-linking adds to this value the contributions of the linking of this chain with each of its translates as provided in the PBC model.

5.3 Eigenvalues of the Periodic Linking Matrix as a Function of Tube Radius and Alignment Constraint

In Figure 7 we show the evolution of the absolute values of the three eigenvalues of a PBC system generated by three independent filaments of length 25. Here, one observes a decreasing tendency in the magnitude of the eigenvalues with increasing tube radius and an increasing tendency with increasing alignment constraint. While one may expect a random system to exhibit a stronger degree of entanglement, we have seen that these filaments have smaller diameter (or squared radius of gyration) thereby offering them a significantly smaller opportunity to entangle with nearby filaments whereas filaments subject to an alignment constraint have a significantly larger number of adjacent filaments with which they may entangle. Thus, we see that the magnitude of the eigenvalues increase with increasing alignment. In addition, for a fixed alignment constraint, the magnitude of the eigenvalues decreases with increasing tube radius across the range of radii presented here, i.e. from 0.1 through 5.0 showing that the filamental structure widely explores the cylindrical tube leading to a decreasing density leading to decreasing entanglement.

5.3.1 Comparison of Systems Across Cross Sectional Scale

Consistent with our earlier analysis, we find that a random system displays the smallest entanglement as measured by the magnitude of the eigenvalues, see Figure 8. In Figure 9 we see that the two eigenvalues of larger magnitudes are rather larger than the random system but tend to get smaller with increasing tube radius while the smallest is relatively stable in magnitude. Since the character of this decrease in the magnitude of the eigenvalues holds across the scale of the alignment constraint, we expect that it is an artifact of the decrease in density of the filaments with increasing tube radius. Considering, in Figure 10, the change in magnitude of the eigenvalues for alignment constraint of 0.85, we do not see any meaningful change in magnitude with increasing tube radius as

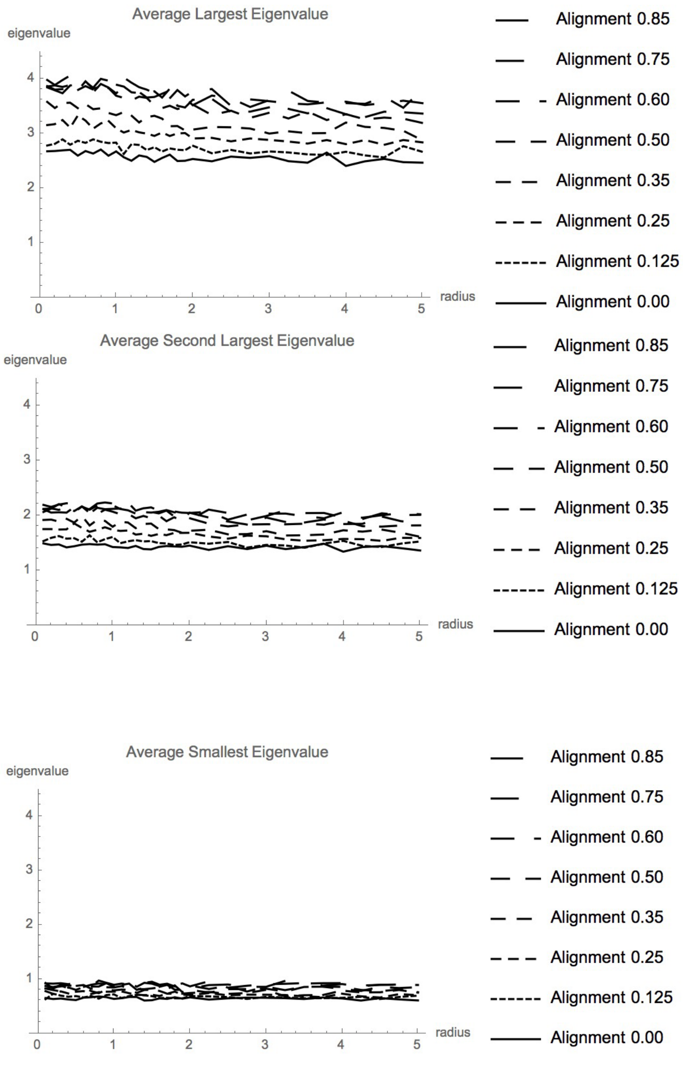

Figure 7: Effect of tube radius and alignment constraint on the mean absolute eigenvalues of a PBC system generated by three independent filaments of length 25

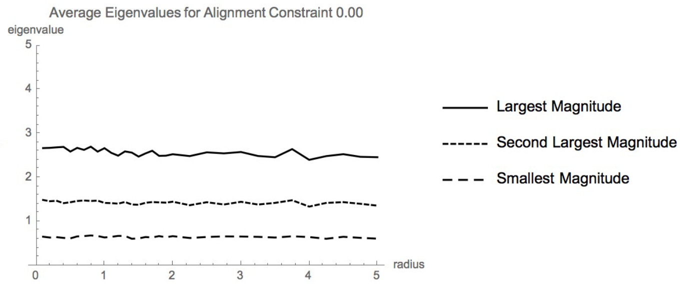

Figure 8: Effect of random alignment, fixed at 0.00, on length 25 filament; radial scale 0.10 to 5.00

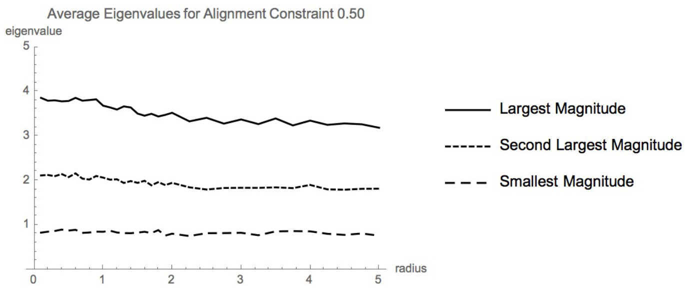

Figure 9: Effect of alignment, fixed at 0.50, on length 25 filament; radial scale 0.10 to 5.00

the magnitudes remain roughly constant at the largest eigenvalue measures of entanglement.

5.3.2 Comparison of Systems Across Degrees of Alignment

We now wish to characterize the consequences of increasing the alignment constraint for a fixed tube radius. For a tube of radius equal to 0.10, 1.00 or 5.00, in Figure 11 we see that there is a visible increase in the magnitude of the largest eigenvalue as the alignment constraint increases independent of the radius of the tube. Indeed, the actual values of the magnitude of the largest eigenvalue are quite similar, independent of the radius of the tube though a bit lower for the very largest tube.

6 Discussion and Conclusions

In this investigation, we have considered short filamental structures confined to tubes of varying cross-sectional radius and subject to varying alignment con-

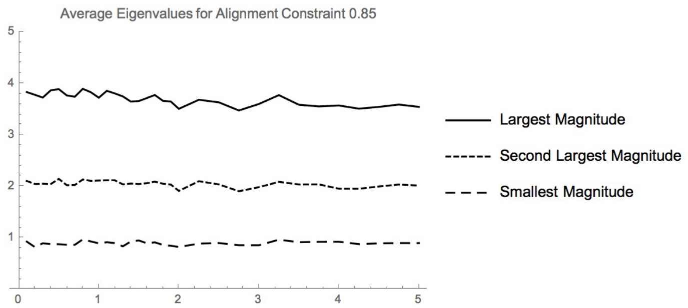

Figure 10: Effect of alignment, fixed at 0.85, on length 25 filament; radial scale 0.10 to 5.00

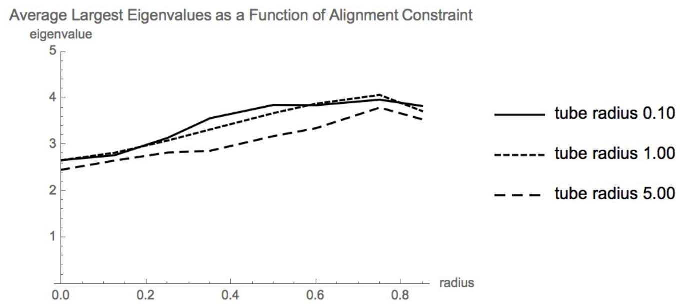

Figure 11: Effect of alignment constraint on the mean largest magnitude eigenvalue for length 25 filaments for tube radii 0.10, 1.00,and 5.00

straints using a periodic boundary condition model. These may be consider as representing vortex flow lines in a fluid or as short polymeric chains in a melt. Employing the associated periodic linking matrix as well as its elements, we show that entanglement occurs across the entire range of cross-sectional radii. We have also shown that entanglement increases with increasing alignment due to the increasingly extended nature of the filamental structure with increasing alignment constraint. As a consequence, we have observed that a randomly aligned structure, according to the eigenvalue measures of the strength of entanglement, is the least entangled.

References

[1] Gauss K F. Zur mathematischen theorie der electrodynamischen wirkungen. *Werke vol 5 Konigl. Ges. Wiss. Gottingen*, page 605, 1877.

[2] W. Kuhn. über die gestalt fadenförmiger moleküle in lösungen. *Kolloid-Zeitschrift*, 68:2–15, 1934.

[3] Henry Keith Moffatt. The degree of knottedness of tangled vortex lines. *Journal of Fluid Mechanics*, 35(01):117–129, 1969.

[4] E Panagiotou. The linking number in systems with periodic boundary conditions. *Journal of Computational Physics*, 2015.

[5] E Panagiotou, KC Millett, and S Lambropoulou. The linking number and the writhe of uniform random walks and polygons in confined spaces. *Journal of Physics A: Mathematical and Theoretical*, 43(4):045208, 2010.

[6] Eleni Panagiotou and Kenneth C Millett. Linking matrices in systems with periodic boundary conditions. *tbd*, tbd(tpd):24, 2016.

[7] Eleni Panagiotou, Kenneth C Millett, and Sofia Lambropoulou. Quantifying entanglement for collections of chains in models with periodic boundary conditions. *Procedia IUTAM*, 7:251–260, 2013.